

Failure Analysis of Fiber Reinforced Composite Materials Used in Malaysian Industries

Jamaluddin Mahmud, Wahyu Kuntjoro & Aidah Jumahat

*Faculty of Mechanical Engineering
Universiti Teknologi MARA (UiTM), Malaysia
Email: jm@salam.uitm.edu.my*

ABSTRACT

The main objective of this paper is to determine the curves bounding the actual load carrying capacity in terms of the First Ply Failure and the Last Ply Failure of composite materials used in Malaysian Industries. A mathematical model and computational model are presented for the analysis. Higher Order Shear Deformation plate theory is employed to predict the deformation of the plate. The selected material properties through thickness is used and accommodated by a discrete layer approach. A program based on finite element method is developed using Fortran-90 to determine the lamina stresses. These stresses are then used in the present failure model to determine the First Ply Failure and Last Ply Failure, by progressively reducing the stiffness of the laminas. Finally, the First Ply Failure and Last Ply failure results are analysed, in terms of lower and upper bound within which the true load carrying capacity lies.

Introduction

In fiber reinforced laminated composite materials, failure in one direction of any single layer implies neither total failure of that layer, nor the whole structure. Load carrying capacity still exists not only in the structure, but also in the layer itself. Therefore, the most common way to deal with failure of a composite laminate is by using two definitions of failure. First Ply Failure (FPF) occurs when initial failure of a single layer in a laminate

fails in any mode of failure. Last Ply Failure (LPF) occurs after the structure has degraded to the point where it is no longer capable of carrying additional load. Therefore, the main objective of this paper is to determine the curves bounding the actual load carrying capacity in terms of the FPF and the LPF of composite materials used in Malaysian Industries.

Literature Review

The most common and oldest method, in terms of finite element analysis for a laminated composite plate, is the standard laminate strength analysis. In 1982, Lee has performed the finite element based failure analysis by using his own direct mode determining failure criterion [1]. The major drawback of a three-dimensional failure analysis is the tremendous amount of memory space and calculation time required. This phenomenon leads to the search for more efficient finite element analysis of composite plates. Reddy and Pandey have developed a first ply failure analysis of composite laminates based on first order shear deformation plate theory [2]. Engblom and Ochoa develop a two-dimensional plate analysis to the above, but with increased interpolation in the through thickness direction [3]. Their analysis is carried out to the last ply failure. Tolson and Zabarar have also developed two-dimensional progressive failure analysis of laminated composite plates, but employing higher order shear deformation theory [4]. Lee's [1] and Hashin's [5] failure criteria are used to determine the mode of failure. However, both criteria neglect the interaction of the coupling effect between the longitudinal stress and the transverse stress. Therefore, the main objective of this research is overcome this deficiency by developing a two-dimensional finite element computational formulation, which could perform the progressive failure analysis of selected fiber reinforced laminated composite plates by employing a failure criterion with interaction terms.

High Order Shear Deformation

Higher order shear deformation theory is developed to improve both the classical lamination theory and the first order shear deformation theory. A higher order term is included in the assumed displacements to describe the warping effect. According to the High-Order Shear Deformation Lamination Theory [6], with θ gradient of displacement and ζ third order derivative of displacement, the assumed displacements are as follows:

$$u(x, y, z) = u_0(x, y) - z\theta_x(x, y) + z^3\xi_x(x, y) \quad (1)$$

$$v(x, y, z) = v_0(x, y) - z\theta_y(x, y) + z^3\xi_y(x, y) \quad (2)$$

$$w(x, y, z) = w_0(x, y) \quad (3)$$

These formulations are employed in the finite-element program to determine the strains and stresses for the laminate analysis. Though the employment of this theory has made the computational analysis to become more complicated, the development of this theory has improved the results, especially for thick plates.

Algorithm for Computation

To determine the strength of a laminated plate, an incremental load analysis procedure is employed [7]. For a given load, the stresses in the material coordinates system for each lamina are calculated. These stresses are then inserted into the failure model to determine if failure has occurred within a lamina of any element. If no failure occurs, the load would be increased to initiate the first failure. When the first ply failure occurs, the stiffness is modified according to the mode of failure.

The plate is meshed and each element has four Gauss points. The failure is checked for one by one layer of a Gauss point in an element. A fiber mode failure at a Gauss point of an element would reduce the stiffness matrix of the failed lamina within that element. Consequently the stiffness, $Q_{11}, Q_{12}, Q_{16}, Q_{55}$ ($\sigma_L, \sigma_{LZ}, \sigma_{LT}$) would be reduced to zero for the failed lamina. A matrix failure at a Gauss point of an element would reduce the stiffness for that element in a different manner, where $Q_{22}, Q_{12}, Q_{16}, Q_{44}$ ($\sigma_T, \sigma_{TZ}, \sigma_{LT}$) would be reduced to zero. If failure were to occur at 1, 2 or 3 Gauss points, the stiffness matrices would be reduced accordingly for that Gauss points. Delamination is the final mode of failure. It is characterised by the interlaminar stresses acting between adjacent layers. An interface of two adjacent layers is identified as delamination failure if either

$$\frac{\sigma_3}{Y} = 1 \quad \text{or} \quad \frac{(\sigma_3^2 + \sigma_4^2)^{1/2}}{S_z} = 1 \quad (4)$$

where S_z is the through-thickness shear strength [8]. A delamination failure at a Gauss point of an element would reduce both laminas adjacent to the delamination, Q_{33}, Q_{44}, Q_{55} ($\sigma_Z, \sigma_{TZ}, \sigma_{LZ}$) to zero. A flow chart of the algorithm described is shown in Figure 1.

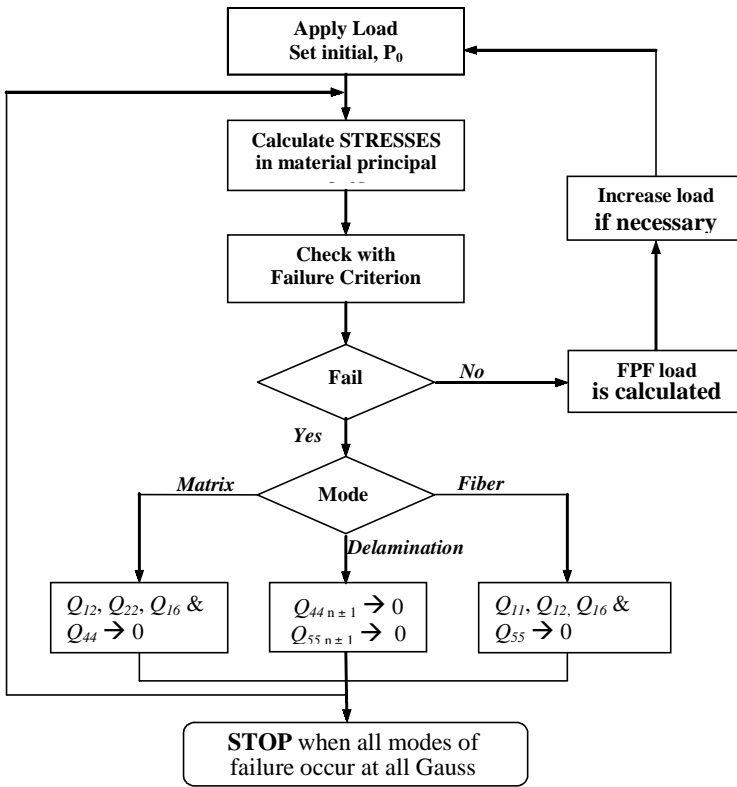


Figure 1: Flow Chart Diagram of the Procedure for the Progressive Failure Analysis

Failure Model

Considering transversely isotropic material [9], the equation used to determine the tensile failure in fiber mode is (with X and Y as the strength in longitudinal and transverse direction, and subscripts T and C denote tensile and compressive mode respectively)

$$\begin{aligned}
 & (1+A) \frac{\sigma_1}{X_T} - \frac{\sqrt{AB}}{X_T Y_T} (\sigma_1 \sigma_2 + \sigma_1 \sigma_3) \\
 & - A \left(\frac{\sigma_1}{X_T} \right)^2 + \frac{1}{S^2} (\tau_5^2 + \tau_6^2) = 1
 \end{aligned} \tag{5}$$

where $A = \frac{X_T}{X_C}$ and $B = \frac{Y_T}{Y_C}$.

The equation [9] used to determine the tensile failure in matrix mode is

$$(1+B)\frac{(\sigma_2+\sigma_3)}{Y_T} - \frac{\sqrt{AB}}{X_T Y_T}(\sigma_1\sigma_2 + \sigma_1\sigma_3) - \frac{B}{Y_T^2}(\sigma_2+\sigma_3)^2 + \frac{\tau_4^2}{R^2} + \frac{1}{S^2}(\tau_5^2 + \tau_6^2) = 1 \quad (6)$$

The equation [9] used to determine the compressive failure in fiber mode is

$$\sigma_1 = X_C \quad (7)$$

The equation [9] used to determine the compressive failure in matrix mode is

$$\left(\frac{1+B}{B}\right)\left(\frac{\sigma_2+\sigma_3}{Y_C}\right) - \frac{1}{\sqrt{AB}}\left(\frac{\sigma_1\sigma_2 + \sigma_1\sigma_3}{X_C Y_C}\right) - \frac{1}{B Y_C^2}(\sigma_2+\sigma_3)^2 + \frac{\tau_4^2}{R^2} + \frac{1}{S^2}(\tau_5^2 + \tau_6^2) = 1 \quad (8)$$

These failure criteria are employed in the analysis to check the progressive failure of the fiber reinforced composite analysis. The advantage of this set of failure criterion is that it relates the strength of the fiber and the strength of the matrix, which ensures better predictions of failure.

Validation of the Numerical Solution

To validate the numerical solutions, the current finite-element formulation is compared with three dimensional elasticity solution and other finite element formulations. The computer program is used to determine the stresses distribution of a 0/90/90/0 laminated composite plate subjected to a sinusoidally distributed transverse load as equation below;

$$P = P_0 (\sin \pi x/a) (\sin \pi y/a) \quad (9)$$

The material properties used for the comparison are those of a graphite-epoxy compound as below;

$$\begin{aligned}
 E_1 &= 25 \times 10^6 \text{ psi} & G_{12} &= 0.5 \times 10^6 \text{ psi} \\
 E_2 &= 1 \times 10^6 \text{ psi} & G_{13} &= 0.5 \times 10^6 \text{ psi} \\
 n_{12} = n_{13} = n_{23} &= 0.25 & G_{23} &= 0.2 \times 10^6 \text{ psi}
 \end{aligned}$$

All plates analysed are square with planar dimension $a \times a$, and total thickness, h . Eight-noded element is used throughout the calculations. The origin of the plate is located at the lower left corner of the midplane. The plate is simply supported [7]. Sample results are presented in Table 1.

Table 1: Comparison of Normalised Displacements

Span to thickness ratio, S	Source	Central deflection, $w^* \left(\frac{a}{2}, \frac{a}{2}, 0 \right)$
4	A – Present finite-element formulation	4.411
	B – Exact elasticity solution [10]	4.491
10	A – Present finite-element formulation	1.671
	B – Exact elasticity solution [10]	1.709
	C – FE formulation of Panda et al. [11]	1.448
20	A – Present finite-element formulation	1.178
	B – Exact elasticity solution [10]	1.189
	C – FE formulation of Panda et al. [11]	1.114
50	A – Present finite-element formulation	1.029
	B – Exact elasticity solution [10]	1.031
	C – FE formulation of Panda et al. [11]	1.016

The displacements reported are stated in their normalised form. This is done to remove the effects of varying loads and changing aspect ratios, $S = a/h$. The normalising equations are as follows:

$$w^* = \frac{w\pi^4\alpha}{12q_0hS^4} \tag{10}$$

$$\text{where } \alpha = \frac{4G_{12} + \{E_1 + E_2(1 + 2\nu_{12})\}}{(1 - \nu_{12}\nu_{21})} \quad (11)$$

Table 1 obviously proves that the displacements obtained using the finite-element solution are close to the exact solution. A detail analysis is done for the case where the aspect ratio of the plate, $S = 10$ to obtain the stresses distributions and compared with results obtained by other researchers [7].

Failure Analysis

Uniaxial Tension

A progressive failure analysis of an angle-ply composite laminate, subjected to uniaxial tensile loading is performed. The analysis is performed using one eight-noded element. The uniaxial model used in the analysis is shown in Figure 2. The plate is square and the length, a , is 20 mm (0.02 m). The laminate is made of E-glass-epoxy having an aspect ratio ($S = a/h$) of 150. Therefore, the thickness of the plate, h , is 1.33333×10^{-4} m and the crosssectional area ($A = ah$) is 2.66667×10^{-6} m². The laminate consists of 24 layers, where the layup studied is $(\theta_4/0_4/-\theta_4)_s$. The material and strength properties for E-glass-epoxy are shown in Table 2.

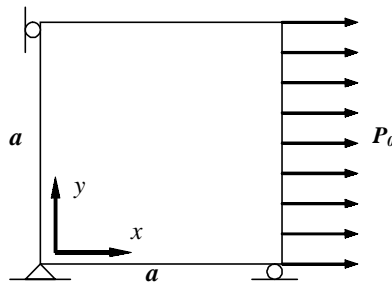


Figure 2: Uniaxial Tension Model

Plate Bending

The computer program is used to investigate the first ply and last ply failure loads of a 0/90/90/0 laminated composite plate [9]. The plate is subjected to a sinusoidally distributed transverse load where $P = P_0(\sin$

Table 2: Material Properties for E-glass-epoxy

$E_1 = 53.78 \text{ GPa}$	$X_T = 1035 \text{ MPa}$
$E_2 = 17.93 \text{ GPa}$	$X_C = 1035 \text{ MPa}$
$\nu_{12} = 0.25$	$Y_T = 27.6 \text{ MPa}$
$G_{12} = 8.62 \text{ GPa}$	$Y_C = 138 \text{ MPa}$
	$S = 41.4 \text{ MPa}$

$\pi x/a)(\sin \pi y/a)$. The plate is square with the dimensions of $a \times a$. The thickness of the plate is h , with the aspect ratio, $S = a/h$. The analysis is performed on different aspect ratios. The aspect ratio is varied from 5 to 100. The length of the plate is 40 mm. Only a quarter of the plate needs to be modelled due to the geometric symmetry of the problem. The plate is simply supported and the boundary conditions are shown in Figure 3.

The material and strength properties for the E-glass/epoxy composite used [7] are the same that is used in uniaxial tension analysis. It is as shown in Table 2 previously. However, for this analysis, sixteen eight-noded elements are used to insure reasonable accuracy in stress calculations. The progressive failure analysis is performed using the present failure model.

Results and Discussion

Uniaxial Tension

The FPF and LPF results are calculated using the finite-element program developed. The exact FPF and LPF loads obtained for variation of fiber

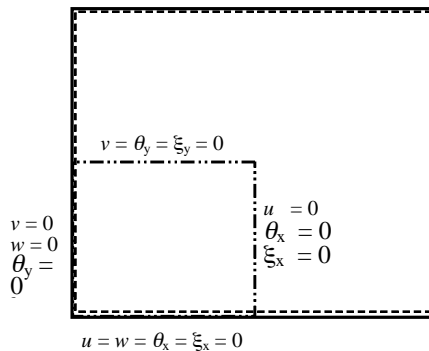


Figure 3: The Boundary Condition for Quarter of a Square Plate

Table 3: First Ply Failure and Last Ply Failure Loads for Uniaxial Tension Analysis

Angle	0°	15°	30°	45°	60°	75°	90°
FPF Load, (N)	1500	720	330	198	144	126	122.4
LPF Load, (N)	1500	730	374	213	270	450	810

orientations are tabulated in Table 3. The table displays the angle of the fiber orientation, the distributed load applied. The stresses are then calculated from the load applied. The orientation of the fiber analysed varies from 0° to 90°, with the step-size of 15°. The corresponding stresses for each FPF and LPF load are calculated and also included in the tables for convenience. The data in Table 3 are used to plot FPF and LPF curves in Figure 4.

Figure 4 shows the FPF and LPF results obtained by using the present finite-element formulation. The curves are plotted to exhibit the stresses for fiber orientation, θ , from 0° to 90° for the E-glass-epoxy laminate. The graphs allow us to visualise and observe the differences of the FPF and LPF curves for the failure analysis by employing the present failure criterion. The region between the FPF and LPF loads reflects the true load carrying capacity for the plate. The result shows that for the fiber orientation from 0° to 45°, the FPF loads and the LPF loads are about the same value. The maximum variation is 13 %. Another interesting observation to point out is that when the fiber orientation is greater than 45°, the FPF and the LPF loads differ progressively. When the fiber

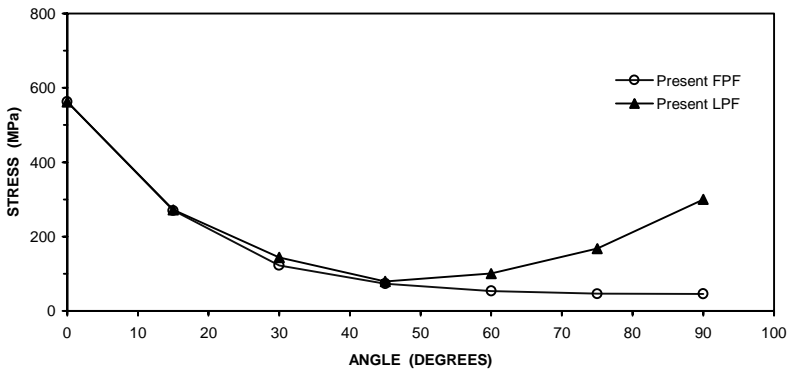


Figure 4: FPF and LPF Curves for E-glass-epoxy Laminate

orientation increases towards 90°, the LPF load diverges from the FPF load value. It is in good agreement with the analysis done previously which were compared with experimental data [9]. This is because the present analysis employs the present criterion, which relates the interaction of the strength between the fibers and the matrices of the laminate. Since the force applied is pulling the plate to the x -direction, the plate is experiencing tension in x -direction and compression in the y -direction. The dominance of the compressive strength of the fiber increases as the angle reaches 90°.

Plate Bending

For the failure analysis of a plate under transverse loading, the results are shown in Table 4.

Table 4: Unnormalised FPF and LPF Loads for the Plate under Transverse Loading

Aspect Ratio, S	5	10	20	50	100
Ply thickness, t_i (mm)	2	1	0.5	0.2	0.1
FPF Load (MPa)	14.6	3.90	1.01	0.23	0.054
LPF Load (MPa)	17.2	7.20	2.69	0.443	0.114

‘Unnormalised Load’ refers to the actual FPF or LPF load, P_0 . Figure 5 shows the First Ply and Last ply failure curves for the 0/90/90/0 laminated as a function of aspect ratio. The failure loads in the graph have been normalised as

$$FPF^* = (FPF)S^2/10^6 \tag{12}$$

$$\text{and LPF}^* = (LPF)S^2/10^6 \tag{13}$$

The normalised FPF loads, FPF^* and LPF loads, LPF^* , are calculated and plotted against the aspect ratio and the graphs are shown in Figure 5. This graph exhibits significantly the true load carrying capacities for the analysed plate. The results converge for the LPF curve but the FPF curve maintains an equal percent difference throughout. This is due to the coupling terms in the present criterion, where the interaction of the stresses in the longitudinal and transverse direction has improved the boundary of the FPF and LPF of the laminate. Figure 5 also shows the FPF and LPF of the E-glass-epoxy compared to Carbon-epoxy composite

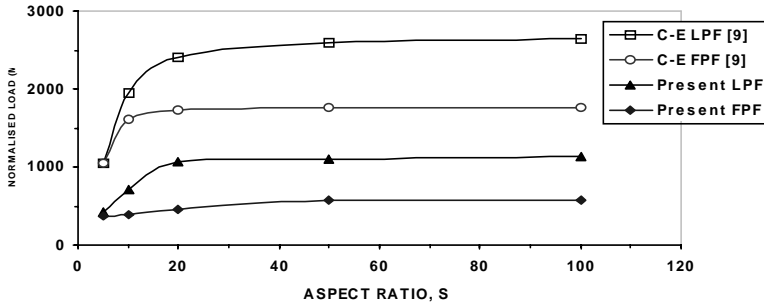


Figure 5: The Normalized FPF and LPF Loads of E-glass-epoxy and Carbon-epoxy

plates. The legend C-E FPF and C-E LPF represents the FPF and LPF curves for composite plates made of Carbon-epoxy [9]. It is obvious that generally, the behaviour of the plates that constitute the failure is the same. However, the loads that fail the Carbon-epoxy plate are much higher than the E-glass-epoxy and this is true based on the material properties compared. The Young's Moduli and the strengths of Carbon-epoxy are much higher than E-glass-epoxy. Finally, we could see that the true loads carrying capacity for Carbon-epoxy in terms of FPF and LPF are much greater than E-glass-epoxy.

Conclusion

This paper presented the application of numerical analysis using Finite Element Method to predict the deformation of composite materials based on the Higher Order Shear Deformation Theory. The stresses are calculated and checked with current failure criteria, which include the coupling terms to predict failure. The failure is analysed in terms of the First Ply Failure and Last Ply Failure to determine the region of the true load carrying capacity. The results of the analysis shown in Table 4 and 5, as well as Figure 4 and 5 shows that the main objective of the research that to perform the failure analysis of fiber reinforced composite materials has been achieved successfully. In ensuring the reliability of the results, before conducting the simulation, the finite-element based program has been validated with exact solutions gained from reliable referred sources, as well as other numerical solutions. The FPF and LPF curves have proven that a single failure in any composite laminate does not constitute

the total failure of the laminate. Though damaged, the laminate could still bear some extra load as long as it does not reach the LPF load. Finally, the results also show that the present failure criterion with the existence of coupling terms, improve the prediction of the progressive failure.

References

- [1] Lee, J. D. 1982. Three Dimensional Finite Element Analysis of Damage Accumulation in Composite Laminate, *Computers and Structures* 15-3, pp. 335-350.
- [2] Reddy, J. N. and Pandey. 1987. A First-Ply Failure Analysis of Composite Laminates, *Computers and Structures* 25, pp. 371-393.
- [3] Engblom, J. J. and Ochoa, O. O. 1987. Analysis of Progressive Failure in Composites, *Composite Science and Technology* 28, pp. 87-102.
- [4] Tolson, S. and Zabarar. 1991. Finite Element Analysis of Progressive Failure in Laminated Composite Plate, *Computers and Structures* 38, pp. 361-372.
- [5] Hashin, Z. 1980. Failure Criteria for Unidirectional Fiber Composites, *Journal of Applied Mechanics* 47, pp. 329-334.
- [6] Pervez, T. 1991. *Transient Dynamic, Damping and Elasto-plastic Analysis of Higher Order Laminated Anisotropic Composite Plates Using Finite Element Method*, Ph. D. Thesis, University of Minnesota, USA.
- [7] Mahmud, J., Kuntjoro, W. and Jumahat, A. 2004. *Failure Analysis of Fiber Reinforced Composite Materials Used in Malaysian Industries*, STG-IRDC UiTM Report.
- [8] Pervez, T. and Abul Fazal, M. A. 1998. Progressive Failure Analysis of Laminated Composite Plates Based on Higher Order Shear Deformation Theory. *Advances in Materials and Processing Technologies, Proceeding of the Fourth International Conference (AMPT 1998)*, pp. 598-611.

- [9] Mahmud, J. 2000. *Failure Analysis of Composite Materials*, Master's Thesis, International Islamic University, Malaysia.
- [10] Pagano, N. J. and Hatfield. 1972. Elastic behaviour of multilayered bi-directional composites, *AIAA Journal*, 10: pp. 931-933.
- [11] Panda, S. C. and Natarajan. 1979. Finite Element Analysis of Laminated Composite Plates, *International Journal for Numerical Methods in Engineering*, 14: pp. 69-79.

